AFM-Investigations , Structural Visualization Studies, and Temperature Optimization of Single Metal Cyclotetraphosphates Synthesized at Elevated Temperature

Khaled M. Elsabawy[a,b]*   , A. El-Maghraby[b,c]

The precursor metal dihydrogen phosphate dihydrate was synthesized by a rapid and simple precipitation method using phosphoric acid, cobalt nitrate at ambient temperature (cobalt(II) was selected as model for metal in these investigations). The precursor was heated and sintered at different temperatures (600, 800, 1000 and 1100 °C) respectively, to optimize the conditions to obtain $Co_2P_4O_{12}$ crystal form with high purity. The products were monitored by both of XRD, IR spectra by additional to accurate imaging via scanning electron microscope (SEM) and AFM-microscope to analyze surface topology and microstructural features of the metal cyclotetraphosphate. Structural investigations via XRD proved that the product obtained at 1100°C is the best and have fine structure with monoclinic structure phase and $C12/c1$ space group with lattice parameter $a = 11.809(2)$, $b = 8.293(1)$, $c = 9.923(2)$ Å, respectively. A visualized investigations were performed to confirm structure validity and stability at sintering temperature (1100 °C) . Visualization studies indicated that variations in bond distances between Co1, Co2, P1 and P2 and different six oxygen atoms (O1 ,O2 , O3 ,O4 ,O5 and O6) inside crystal lattice are responsible for increasing lattice flexibility factor (by controlling in shrinkage and expansion coefficient) and consequently increase its bonds stability to break .

* Corresponding Authors
    E-Mail: ksabawy@yahoo.com
[a]   Materials Science Unit , Chemistry Department ,Faculty of Science,Tanta University-31725-Tanta–Egypt
[b]   Department of Chemistry, Faculty of Science, Taif University, 888- Taif, Kingdom of Saudi Arabia
[c]   Ceramic Department, Chemistry Unit, National Research Center, Dokki, Tahrir st., Egypt

Introduction

In the last decade, synthesis and structures of inorganic phosphates at micro-/nanoscale levels is a significant challenge, which attracts increased attention because of their strong influence on the chemical and physical properties of materials.[1-3]

Morphology influences not only the intrinsic chemical, optical, and catalytic properties of micro/nano scale metal phosphates, but also their relevant applications in electronic, biocompartible and biodegradable in tissue.[2,4]

As one of the members of phosphate material family, transition metal cyclotetraphosphate micro-/nanoparticles can be used as potential pigments, selective catalysts, phosphors, materials for corrosion-resistant coatings and biocompartible and biodegradable in tissues.[5-8] Several bivalent including 3d metals, namely, Mn, Co, Fe, Zn, Cu, and Ni, are known to form the single metal cyclotetraphosphate $M_2P_4O_{12}$, where M(II) stands for a bivalent metal. The binary metal cyclotetraphosphates $M_{2-x}A_xP_4O_{12}$ (M and A=Mg, Ca, Mn, Co, Ni, Zn, or Cu; x=0–2), isostructural with the single metal cyclotetraphosphates $M_2P_4O_{12}$, were prepared by Trojan et al.[5-8] and Boonchom et al.[9-11] All these compounds have similar X-ray diffraction patterns and close unit cell parameters, which crystallize in monoclinic space group

$C2/c$ (Z=4).[12] Various methods have been employed to synthesize binary metal cyclotetraphosphates, including two-step thermal method,[5-8] hydrothermal synthesis[5] and the decomposition of binary metal(II) dihydrogenphosphates $(M_{1-y}A_y(H_2PO_4)_2.nH_2O$; where M and A=Ca, Mg, Mn, Fe, Co, Ni, Cu or Zn; y=0–1; n=1–4).[9-11] This work is of immense interest because it appears economically advantageous to replace partially the divalent metal cations by some cheaper bivalent element which could also improve special properties as above mentioned.[1-4] However, it is relevant to synthesize binary cyclotetraphosphate and its solid solution because changing the metal ratio influences its useful properties. Consequently, it is a major challenge to synthesize binary metal cyclotetraphosphate micro/nano particles with its intrinsic shape-dependent properties and resulting application. Recently, cobalt iron pyrophosphate $CoFeP_2O_7$ and cobalt iron cyclotetraphosphate $CoFeP_4O_{12}$ were prepared by mixing of $CoCO_3$, Fe and H_3PO_4 in water–methanol and in water– acetone, respectively.[13,14]

The difference of media (solvents) in the precipitation process leads to obtain different phosphates, as revealed by XRD and FTIR data. Due to its solubility in water and its ability to associate with metal ions in media, solvent has been used as a binder cum gel for shaping materials (bulk, porous, micro- or nano particles) and a matrix for entrapment of ions to generate a gelled precursor which resulted in obtaining different material or same material with different size and morphology after heat treatment. The results obtained are also in agreement with other phosphate group reported in literature.[15,16]

The major objective of the present investigations is understanding the role of structural parameters within crystal lattice of $M_2P_4O_{12}$ that stabilize structure of crystal even at elevated temperatures. Furthermore understanding the structural parameters effects on the morphological and surface nature of metalized cyclotetraphosphates.

Experimental

Synthesis of metal cyclotetraphosphates

The cobalt cyclotetraphosphate was synthesized via three step reactions. First reaction is dissolving cobalt carbonate in few drops of concentrated nitric acid forming acidic cobalt nitrate then solution neutralized by condensed ammonia solution. The second step is the reaction with 70% phosphoric acid forming cobalt dihydrogen phosphate at temperature 230 °C, the third step is heating followed by sintering process at 1100 °C to form violet powder from pure cobalt cyclotetraphosphate. These steps are in partial agreement with the method of Parada et al.[5]

$$M^{II}CO_3 + HNO_3 \rightarrow M(NO_3)_2 \qquad (1)$$

$$M(NO_3)_2 + 2H_3PO_4 \rightarrow M(H_2PO_4)_2 + H_2O + NO_2 \qquad (2)$$

$$M(H_2PO_4)_2 \rightarrow M_2P_4O_{12} \qquad (3)$$
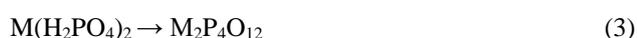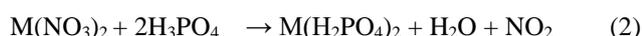
where M=Co. The violet powder from pure cobalt cyclotetraphosphate was grounded in agate mortar for 15 min, then the resulted powder forwarded to perform the different structural measurements.

Structural measurements

The X-ray diffraction (XRD) measurements were carried out at room temperature on the fine ground samples using Cu-Kα radiation source, Ni-filter and a computerized STOE diffractometer/Germany with two θ step scan technique. Rietveld refinement and indexing of structure were made via Fullprof package and Gesas program.

A visualized studies of crystal structure were made by using Diamond Molecular Structure version 3.2 package, Germany and MERCURY-2.3 depending up on single crystal structural data of pure cobalt cyclotetraphosphates including atomic coordinates of monoclinic phase supplied from ICSD–Karlsruhe-Germany. Scannig electron microscopy (SEM) measurements were carried out along ab-plane using a small pieces of the prepared samples by using a computerized SEM camera with elemental analyzer unit Shimadzu (Japan). Atomic force microscopy (AFM): High-resolution Atomic Force Microscopy (AFM) is used for testing morphological features and topological map (Veeco-di Innova Model-2009-AFM-USA). The applied mode was tapping non-contacting mode. For accurate mapping of the surface topology AFM-raw data were forwarded to the Origin-Lab version 6-USA program to visualize more accurate three dimension surface of the sample under investigation. This process is new trend to get high resolution 3D-mapped surface for very small area.

A visualization study made is concerned by matching and comparison of experimental and theoretical data of atomic positions, bond distances, oxidation states and bond torsion on the crystal structure formed. Some of these data can be obtained free of charge from The Cambridge Crystallographic Data Centre via www.ccdc.cam.ac.uk/data_request/cif, or by emailing data_request@ccdc.cam.ac.uk, or by contacting ICSD-Fiz-Karlsruhe-Germany.

FT-Infrared Spectroscopy

The infrared spectra of the solid products obtained were recorded from KBr discs using a Shimadzu FT-IR Spectrophotometer in the range from 400 to 4000 cm^{-1}.

RESULTS AND DISCUSSION

Structural Identification

Fig.1 displays different x-ray diffraction patterns of cobalt cyclotetraphosphate at different sintering temperatures (600, 800, 1000 and 1100 °C) respectively. The accurate analyses of these patterns were performed by using both of Rietveld and indexing via Fullprof package and Gesas program. The analysis is focused on the main intense reflection peaks (fingerprint of structure) and indicated that cobalt cyclotetraphosphate is mainly belong to single monoclinic phase with $C12/c_1$ space group as symbolized by pink cycles in Fig.1 and only very few percentage of cobalt oxide as secondary phase in minor. It was observed that the impurity phases are decreasing as sintering temperatures are increasing as shown in Fig.1 where impurity phases are assigned by blue squares. The comparisons of most intense reflections peaks in all patterns (fingerprint reflections represent monoclinic–phase) indicated that cobalt cyclotetraphosphate, which is sintered at 1100 °C is the best fit one with high purity than others which sintered at temperatures 600, 800 and 1000 °C, respectively.
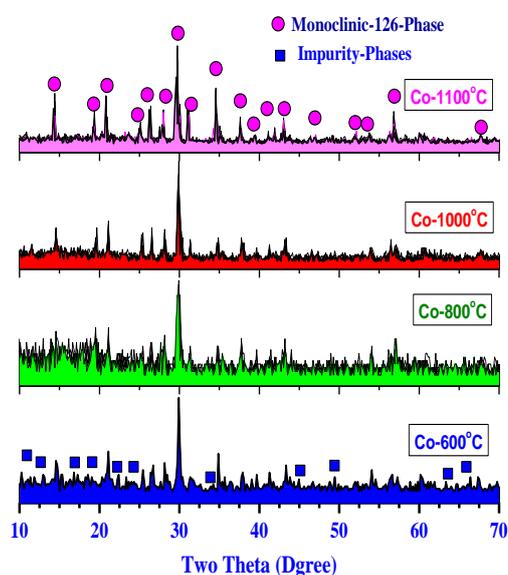
Figure 1. X-ray diffraction patterns of cobalt cyclotetraphosphate formed at different sintering temperatures (600, 800, 1000 and 1100°C) respectively.

In the hypothesis of isostructural, due to existence of cobalt(II) and cobalt(III) the spectrum peaks for the system of cobalt cyclotetraphosphate (solid solution) which is single metal cyclotetraphosphate ($M_2P_4O_{12}$, M=Co) are quite similar because of the equivalent electronic charges and the close radii of cations. Consequently, all the diffraction peaks in the Fig.1 are found to be in a good agreement with monoclinic $M_2P_4O_{12}$ and space group C12/c1 without violation. Only a few characteristic peaks of other impurities

(e.g.Co-Oxide) was clearly observed at lower sintering temperatures (600, 800°C).

From XRD analysis (Fig. 1), grain size evaluated and calculated according to the Scherrer's formula: $D=K\lambda/(\beta cos\theta)$, where D is particle diameter, K=0.89 (the Scherrer's constant), λ=1.5406 (wavelength of the X-ray used), β is the width of line at the half-maximum intensity and θ is the corresponding angle. The average crystallite size of product is estimated from the strongest three diffraction peaks below 40° for 2θ and found to be 98±11 nm. This crystal size of the prepared cobalt cyclotetraphosphate is smaller than those of data estimated from SEM and AFM-investigations in the present work which confirms that the powder mixture of cobalt cyclotetraphosphate is not unified grain sizes and grain sizes are varied in the bulk than surface's layers. The lattice parameters were calculated from the XRD spectra and found to be a=11.809(2), b=8.293(1), c=9.923(2) Å ,which are very close to those of the standard data file (ICSD #300027) and the literatures also.[9-11,14]

FT-IR-Spectroscopic Investigations

Fig. 2 displays infrared spectra recorded for $Co_2P_4O_{12}$ (126-Phase $=AB_2X_6$ structure type) after heating process and sintering at 1100 °C . The most intense reflection pear of IR-spectra are assigned by red cycles as clear in Fig. 2. It is well known that the $Co_2P_4O_{12}$ structure is mainly characterized by a three- dimensional framework with MO_6 (M=Co) polyhedral linked with P_4O_{12} rings by M–O–P. The basic structure unit is the centrosymmetric cyclo-tetraphosphate ring P_4O_{12} and therefore vibrational modes can consider it as made up of the $[P_4O_{12}]^{4-}$ anion. The different vibrational modes of $[P_4O_{12}]^{4-}$-ion observed in the frequency range of 370–1400 cm^{-1} are assigned according to the literature.[17-19]

$[PO_2]^{2-}$ radical and the P–O–P bridge which differs in their bond strength and as a result multi-splitting processes are occurred as shown in Fig. 2. As the P–O bond strength in the $[PO_2]^{2-}$ radical is stronger than in the P–O–P bridge, the stretching frequencies of the $[PO_2]^{2-}$ radical are expected to be higher than those in the P–O–P bridge. The P–O bonds in the $[PO_2]^{2-}$ radical show its asymmetric and symmetric stretching frequencies around 1327–1237 and 1150–1000 cm^{-1}, respectively.

The asymmetric and symmetric stretching frequencies of the P–O–P bridge are observed in the regions of 1000–900 and 800–700 cm^{-1}, respectively. The symmetric P–O–P bridge stretching modes occur at 736 and 714 cm^{-1}. These observed bands are known to be the most striking feature of cyclotetraphosphate spectra, along with the presence of the v_{as}(OPO) band. From X-ray diffraction data,[12] it was shown that the crystal structure is monoclinic (space group $C2/c1$) with a cyclic structure of the $[P_4O_{12}]^{4-}$ anion. This has been confirmed by the IR measurements. The bending modes are expected in the area 600–400 cm^{-1} $[PO_2]^{2-}$ radical) and 400–370 cm^{-1} (P–O–P bridge). The metal–O stretching usually appears in the bending mode region as the bending modes of the P–O–P bridge and absorption bands associated with these vibrations are usually very weak. The weak IR band at 400 cm^{-1} is probably due to metal–oxygen (Co-O) stretching mode.

Scanning Electron Microscopy (SEM) and EDX-Elemental Analysis (EDX)

Fig. 3a shows scanning electron micrograph recorded for cobalt cyclotetraphosphate synthesized at 1100 °C, it is so difficult to observe inhomogeneity within the micrograph due to that the powders used are very fine and the grain size estimated is too small.
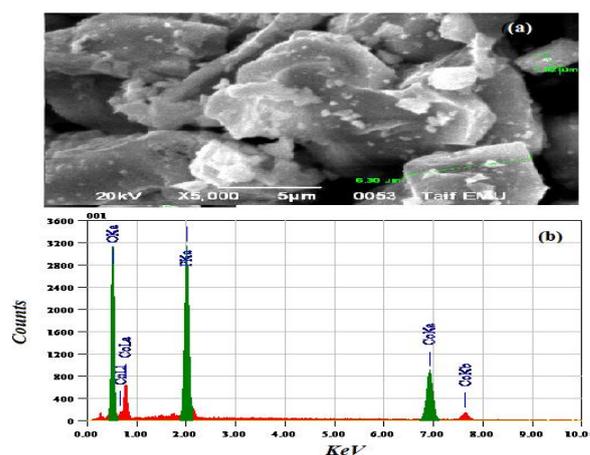
Figure 3. Scanning electron micrograph recorded for cobalt cyclotetraphosphate synthesized at 1100°C with average grain size ranged in between 3.2-3.78 μm.

Figure. 2. Infrared spectra recorded for $Co_2P_4O_{12}$ (126-Phase $=AB_2X_6$ structure type) after firing process and sintering at 1100 °C .

The peaks splitting in these regions is due to the different strength of the bond between cations (M= Co^{2+} or Co^{3+}) and anion $[P_4O_{12}]^{4-}$, which confirms the inserting different cations in the skeletal as well as the formation of multi-valence cobalt(II,III) cyclotetraphosphate also as confirmed in the visualization studies part. The anion contains the

The average grain size was estimated from SE-micrograph and found to be ranged in between 3.2-3.78 μm which is relatively high in contrast with data estimated from XRD through Scherrer's equation (D=0.98 μm). This indicates that the actual grain size in the material bulk could be smaller than that detected on the surface morphology.

Furthermore, in our EDX (energy disperse X-ray) analysis as shown in Fig. 3b and Table 1a, the molar ratios of cobalt cyclotetraphosphate was detected qualitatively with very good fitting to the actual molar ratio(1:2:6) as shown in Table 1a (Supplementary material).

The EDX examinations were performed on random spots within the same sample to confirm accuracy of calculations molar ratios of cobalt cyclotetraphosphate as possible .

Atomic Force Investigations (AFM) :

Fig.4 shows 3D-AFM-micrograph tapping mode image trapped for scanned area 0.1 μm^2 of cobalt cyclotetraphosphate (Co$_2$P$_4$O$_{12}$).The image was constructed by application tapping mode with slow scan rate and high resolution imaging with 1024 line per 0.1 nm.The tapping amplitude current was monitored as a function of line drawing heights. For more accurate surface analysis AFM-raw data was forwarded to Origin Lab program version 7 and the data are converted into matrix then 3D-contour surface mapping is constructed as shown in Fig.5a.
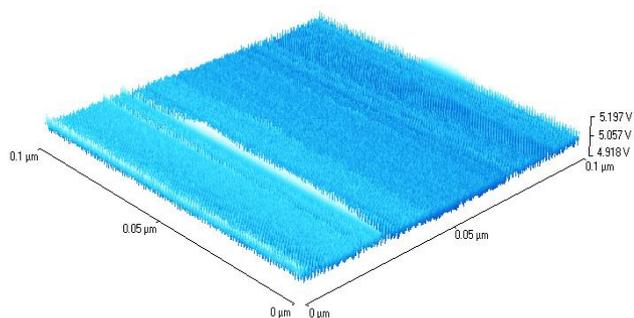
Figure 4. 3D-AFM-micrograph tapping mode image recorded for scanned area 0.1 μm^2 of cobalt cyclotetraphosphate (Co$_2$P$_4$O$_{12}$).

Fig.5a displays 3D-visualized-contour plot of AFM-micrograph surface image trapped for scanned area 0.2 μm^2 of cobalt cyclotetraphosphate (Co$_2$P$_4$O$_{12}$). To increase the accuracy of analysis of this image the data were forwarded to plot Fig.5b which is 2D-visualized-contour plot of the same image of cobalt cyclotetraphosphate (Co$_2$P$_4$O$_{12}$). The analysis of the surface nature and morphology enrich us to understand application of such these materials metal cyclotetraphosphate (M$_2$P$_4$O$_{12}$) as colorant materials in coating and ceramic industry .

The AFM-tapping mode trapped image can be divided into three zones 1st zone include (yellow, orange and red color) this zone represents ~21% of the whole scanned area which is equal ~ 0.042 μm^2 ,the surface heights in this zone ranged in between 6.072-6.14 μm as clear in the key-image .The red zone represents 2%=0.004 μm^2 which processes the highest height on the scanned area with height$_{max}$=6.14 μm. The second zone represents ~ [dark green zone (23%) + pale green zone (18%)] which represents ~ 41% (0.082 μm^2) from the whole scanned area with heights gradient ranged in between 6.027-6.06 μm .
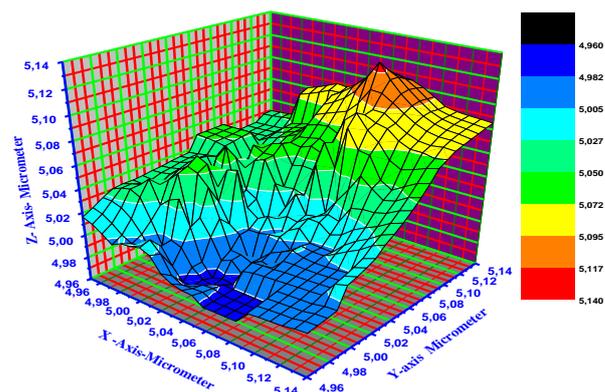
Figure 5a. 3D-visualized-contour plot of AFM-micrograph surface image recorded for scanned area 0.2 μm^2 of cobalt cyclotetraphosphate (Co$_2$P$_4$O$_{12}$).
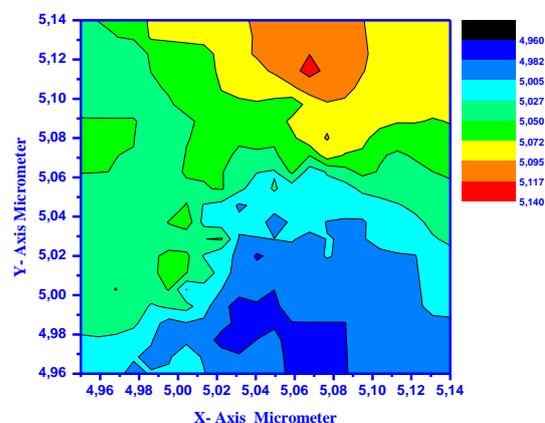
Figure 5b. 2D-visualized-contour plot of AFM-micrograph tapping mode image recorded for scanned area 0.2 μm^2 of cobalt cyclotetraphosphate (Co$_2$P$_4$O$_{12}$).

The 3rd zone occupies ~ 38% = 0.076 μm^2 from the whole scanned area with heights gradient lies in between 4.88-6.06 μm. The average grain size was estimated from AFM-analysis and found in between 56-80 nm which is nearly matched with that calculated from XRD by applying Scherrer's formula (~98 nm). The differences in the values of average grain sizes calculated via SEM, AFM and Scherrer's formula are good evidence for existence gradient in the grain sizes in the bulk which are completely different than those on the surface layers.

Structural Visualization Studies

Fig. 6 displays the unit cell of cobalt cyclotetraphosphate which built up via DIAMOND IMPACT CRYSTAL PROGRAM version 3.2 depending up on the single crystal data and atomic coordinates locations of pure cobalt cyclotetraphsphate. The unit cell was visualized and built up with minimum 138 atoms (Co=16, P=38 and O=94 atoms) and four edges. A visualization study made is concerned by matching and comparison of experimental and theoretical data of atomic positions, bond distances, oxidation states and bond torsion on the crystal structure formed .

Table.1. Selected bond lengths and angles inside crystal lattice of $Co_2P_4O_{12}$

Atom1	Atom2	d_{1-2} Å	Atom3	d_{1-3} Å	Angle 312
Co1	O1	2.0927	O1	2.0927	180.000
	O1	2.0927	O2	2.3366	82.238
	O1	2.0927	O2	2.3366	97.762
	O2	2.3366	O2	2.3366	180.000
	O2	2.3366	O5	2.4865	116.323
	O5	2.4865	O3	2.8210	57.061
	O5	2.4865	P1	3.0353	157.072
	O3	2.8210	O3	2.8210	180.000
	O3	2.8210	P2	2.9164	144.014
	P2	2.9164	P2	2.9164	180.000
	P2	2.9164	P1	3.0353	71.568
	P2	2.9164	O4	3.5270	29.627
	P2	2.9164	O6	3.5756	80.753
	P1	3.0353	P1	3.0353	180.000
	P1	3.0353	O6	3.5756	21.363
	O4	3.5270	O6	3.5756	96.488
	O4	3.5270	O6	3.5756	83.512
	O6	3.5756	O6	3.5756	180.000
	O6	3.5756	P2	3.6583	79.758
	O6	3.5756	P2	3.6583	100.242
Co2	O6	2.1694	O6	2.1694	93.593
	O6	2.1694	O5	2.3208	84.836
	O6	2.1694	O5	2.3208	174.602
	O6	2.1694	O2	2.5737	112.127
	O6	2.1694	O2	2.5737	71.914
	O5	2.3208	O4	3.5398	76.791
	O5	2.3208	P2	3.7464	74.787
	O5	2.3208	P2	3.7464	116.925
	O5	2.3208	O3	3.9043	138.211
	O5	2.3208	O3	3.9043	120.351
	O2	2.5737	O2	2.5737	174.457
	O2	2.5737	P1	3.1577	77.031
	O2	2.5737	O6	3.3434	98.404
	O2	2.5737	O6	3.3434	80.635
	P1	3.1577	O4	3.5398	93.099
	P1	3.1577	O3	3.9043	107.617
	P1	3.1577	O3	3.9043	136.556
	O6	3.3434	O6	3.3434	160.281
	O6	3.3434	P1	3.4087	138.822
	P1	3.4087	P1	3.4087	79.006
	P1	3.4087	O1	3.5271	84.012
	P1	3.4087	O1	3.5271	67.309
	P1	3.4087	O4	3.5398	103.558
	O1	3.5271	P2	3.7464	25.747
	O1	3.5271	P2	3.7464	144.026
	O1	3.5271	O3	3.9043	56.224
	O1	3.5271	O3	3.9043	87.439
	O4	3.5398	O4	3.5398	88.346
	O4	3.5398	P2	3.7464	74.116
	O4	3.5398	P2	3.7464	118.697
	P2	3.7464	O3	3.9043	72.236
	P2	3.7464	O3	3.9043	91.882
	P2	3.7464	O3	3.9043	91.882
	P2	3.7464	O3	3.9043	72.236
	O3	3.9043	O3	3.9043	37.949

Table.2. Selected bond lengths and angles inside crystal lattice of $Co_2P_4O_{12}$

Atom1	Atom2	d_{1-2} Å	Atom3	d_{1-3} Å	Angle 312^
P1	O5	1.2222	O6	1.3354	112.012
	O5	1.2222	O3	1.8394	111.327
	O5	1.2222	O4	1.9623	98.852
	O5	1.2222	Co1	3.0353	52.425
	O6	1.3354	O1	3.8450	71.883
	O6	1.3354	O6	3.9043	47.653
	O1	3.4635	O1	3.9266	106.380
	O1	3.4635	O2	3.9527	25.309
	O1	3.4635	P1	3.9812	156.181
	O3	1.8394	Co1	3.0353	65.455
	O3	1.8394	Co2	3.1577	148.445
	O4	1.9623	O1	3.9266	47.041
	O4	1.9623	O2	3.9527	87.564
	O4	1.9623	P1	3.9812	64.088
	Co1	3.0353	Co2	3.1577	83.872
	Co1	3.0353	O3	3.3910	107.797
	Co1	3.0353	Co2	3.4087	90.253
	Co2	3.1577	P2	3.4815	133.588
	Co2	3.1577	O1	3.5216	76.412
	O3	3.3910	O1	3.8450	90.375
	Co2	3.4087	O1	3.9266	108.957
	Co2	3.4087	O2	3.9527	40.078
	O2	3.5532	O2	3.9527	62.931
	O2	3.5532	P1	3.9812	152.445
	O3	3.4278	P2	3.4815	82.722
	P2	3.4815	O1	3.5216	59.248
	P2	3.5485	O2	3.5982	110.496
	O4	3.5878	O2	3.5982	95.547
	O4	3.5878	O1	3.8450	84.205
	O4	3.5878	O6	3.9043	96.550
	O4	3.5878	O1	3.9266	72.730
P2	O2	1.3584	O1	1.6346	90.263
	O2	1.3584	O4	1.7500	122.795
	O1	1.6346	O5	3.8101	159.446
	O1	1.6346	O4	3.8181	47.186
	O1	1.6346	O5	3.8547	102.964
	O4	1.7500	O3	1.7746	85.307
	O4	1.7500	Co1	2.9164	94.901
	O3	1.7746	O5	3.8101	34.432
	O3	1.7746	O5	3.8547	105.956
	Co1	2.9164	O5	3.4562	164.249
	Co1	2.9164	O1	3.4618	37.075
	O5	3.4562	O4	3.8181	61.446
	O5	3.4562	O5	3.8547	151.691
	O1	3.4618	P1	3.4815	60.953
	O1	3.4618	P1	3.5485	68.115
	P1	3.5485	O5	3.8101	69.465
	P1	3.5485	O4	3.8181	128.505
	P1	3.5485	O5	3.8547	127.918
	O6	3.5725	O3	3.5777	169.950
	O6	3.5725	Co1	3.6583	84.063
	O3	3.5777	O4	3.8181	51.319
	O3	3.5777	O5	3.8547	130.744
	Co1	3.6583	O2	3.7104	36.966
	Co1	3.6583	O1	3.7128	122.659

Table 2 (cont.)

Atom1	Atom2	d_{1-2} Å	Atom3	d_{1-3} Å	Angle 312
P2	O5	3.6692	O5	3.8547	147.193
	O2	3.7104	O1	3.7128	156.019
	Co2	3.7464	O5	3.8547	35.519
	O5	3.8101	O4	3.8181	112.308

Table.3. Selected bond lengths and angles inside crystal lattice of $Co_2P_4O_{12}$.

Atom1	Atom2	d_{1-2} Å	Atom3	d_{1-3} Å	Angle 312
O1	P2	1.6346	Co1	2.0927	157.754
	P2	1.6346	O2	2.1302	39.621
	P2	1.6346	P1	3.9266	82.859
	Co1	2.0927	O2	2.1302	151.780
	Co1	2.0927	O5	2.6771	61.400
	O2	2.1302	O6	3.6570	81.232
	O2	2.1302	P2	3.7128	114.101
	O2	2.9186	O4	2.9451	75.146
	O2	2.9186	O4	2.9609	129.658
	O4	2.9451	O5	3.7359	138.844
	O4	2.9451	O6	3.7769	69.906
	O3	3.0569	O2	3.3406	135.391
	O3	3.0569	P2	3.4618	113.44
	O2	3.3406	P1	3.9266	79.250
	P2	3.4618	O3	3.5075	29.494
	O3	3.5174	O3	3.8471	157.065
	O3	3.5174	P1	3.9266	159.635
	P1	3.5216	Co2	3.5271	163.460
	P1	3.5216	O6	3.6570	129.656
	Co2	3.5271	P1	3.9266	118.457
	O6	3.6570	P2	3.7128	70.152
	P2	3.7128	P1	3.9266	148.032
	O5	3.7359	O6	3.7769	79.868
	O5	3.7359	P1	3.8450	18.483
	O5	3.7359	O3	3.8471	140.930
	O5	3.7359	P1	3.9266	120.490
	O6	3.7769	O3	3.8471	138.211
	O6	3.7769	P1	3.9266	141.255
	P1	3.8450	O3	3.8471	159.386
	O3	3.8471	P1	3.9266	27.350
O2	P2	1.3584	O1	2.1302	50.116
	P2	1.3584	Co1	2.3366	100.899
	O1	2.1302	O6	3.8732	144.603
	O1	2.1302	O6	3.9416	66.484
	O1	2.1302	P1	3.9527	94.733
	Co1	2.3366	O5	2.5475	61.027
	O5	2.5475	O6	3.8732	30.571
	O5	2.5475	O6	3.9416	84.546
	Co2	2.5737	O6	3.9416	30.654
	Co2	2.5737	P1	3.9527	58.507
	O3	2.6359	O4	2.7355	52.758
	O3	2.6359	O6	2.8042	141.814
	O4	2.7355	O6	3.9416	116.394
	O4	2.7355	P1	3.9527	78.086
	O6	2.8042	O1	2.9186	126.931
	O6	2.8042	O1	3.3406	83.218

Table 3 (cont.)

Atom1	Atom2	d_{1-2} Å	Atom3	d_{1-3} Å	Angle 312
O2	O6	2.8042	O4	3.5756	115.388
	O6	2.8042	P1	3.5982	63.049
	O6	2.8042	P2	3.7104	126.522
	O6	2.8042	O6	3.9416	52.695
	O6	2.8042	P1	3.9527	11.746
	O1	2.9186	O1	3.3406	83.639
	O1	2.9186	O4	3.5756	52.764
	O1	2.9186	P1	3.5982	64.434
	O4	3.5756	O6	3.9416	73.486
	P1	3.5982	P2	3.7104	73.993
	P1	3.5982	O6	3.8732	20.160

Many researchers in the past did their best to understand the crystallographic structure of phosphates (open phosphates or cyclic poly phosphates).[20-28]

The initial analysis of structural parameters inside visualized crystal lattice of cobalt cyclotetraphosphate indicated that there are two different types of cobalt, namely (Co1 and Co2). Two types of phosphorous atoms (P1 and P2) and finally six different types of oxygen atoms namely (O1, O2, O3, O4, O5 and O6).

The comparison between visualized XRD-profile (Supplementary material) and the experimental XRD-pattern sintered at 1100 °C Fig. 1, indicated that there is type of fitting coupled with high figure of merit between both patterns specially on the point of view positions of most intense reflection peaks on both patterns .The shifts on some intense reflection peak position within limits of two theta values ~2 degree could due to impurity phases interactions with the main monoclinic structure of cobalt cyclotetraphosphate on the experimental pattern. Fig.7 displays the regular distribution of PO_3-polyhera throughout the unit cell of cobalt cyclotetraphosphate .The analysis of these polyhedron indicated that the phosphorous atom as central ion was surrounding by oxygen atoms , three oxygen atoms represents the triangle base lie at nearly the same distance from phosphorous (central metal ion) while the forth one at distance longer than the others three oxygen of triangle base .

The accurate analysis of bond lengths , torsion on angles inside the crystal lattice of cobalt cyclotetraphosphate (Tables 1-3) may enrich us understand that what are the structural factors responsible for lattice stability .

The analysis of data in Tables 1, 2 and 3, one can conclude the following observations; cobalt type one symbolized as (Co1) was linked with all types of oxygen atoms recording the following bond lengths (2.0927, 2.3366, 2.8210, 3.5270, 2.4865 and 3.5756 Å) corresponding to Co1-O1, Co1-O2, Co1-O3, Co1-O4, Co1-O5 and Co1-O6 bond lengths respectively .From these observations one can conclude that O1, O2 and O3 could be located as triangle base of PO_3^- while O4, O5 and O6 can be oriented as axial oxygen to complete the vacant site of tetrahedron forming PO_4^- -anion .The cobalt type one (Co1) is also linked with two different types of phosphorous namely (P1 and P2) with bond

Table.3. (cont.)

Table 3. (cont.)

Atom1	Atom2	d_{1-2} Å	Atom3	d_{1-3} Å	Angle 312^
O3	P2	1.7746	P1	1.8394	148.861
	P2	1.7746	O4	2.3882	46.911
	P1	1.8394	O4	3.2099	33.597
	P1	1.8394	O6	3.3713	92.284
	P1	1.8394	P1	3.3910	108.337
	O4	2.3882	P2	3.5777	102.290
	O4	2.3882	O3	3.7969	57.227
	O4	2.3882	O1	3.8471	88.198
	O3	2.5389	O5	2.5520	126.753
	O3	2.5389	O6	2.5691	82.598
	O3	2.5389	O2	2.6359	123.991
	O5	2.5520	Co1	2.8210	54.856
	O5	2.5520	O1	3.0569	146.390
	O6	2.5691	O4	3.2099	55.840
	O2	2.6359	O6	3.3713	98.001
	O2	2.6359	P1	3.3910	99.094
	O2	2.6359	P1	3.4278	99.516
	O2	2.6359	O5	3.4479	108.342
	Co1	2.8210	O4	3.2099	103.234
	Co1	2.8210	O6	3.3713	102.506
	O1	3.0569	P1	3.4278	89.823
	O4	3.2099	P1	3.3910	112.702
	O4	3.2099	P1	3.4278	65.342
	O4	3.2099	O5	3.4479	68.024
	O4	3.2099	O1	3.5075	83.165
	O4	3.2099	O1	3.5174	119.071
	O6	3.3713	O1	3.8471	97.213
	P1	3.3910	P1	3.4278	131.958
	P1	3.3910	O5	3.4479	111.574
	O5	3.4479	O1	3.8471	42.620
	O5	3.4479	Co2	3.9043	143.431
	O1	3.5075	O1	3.5174	73.138
	O1	3.5075	P2	3.5777	142.989
	O3	3.7969	O1	3.8471	54.622
	O3	3.7969	Co2	3.9043	123.375
	O1	3.8471	Co2	3.9043	100.918
O4	P2	1.7500	P1	1.9623	145.774
	P2	1.7500	O3	2.3882	47.781
	P1	1.9623	O5	3.7632	92.572
	P1	1.9623	P2	3.8181	82.582
	P1	1.9623	O6	3.9110	148.016
	O3	2.3882	O5	2.4663	90.497
	O3	2.3882	O2	2.7355	61.479
	O3	2.3882	O6	3.9110	106.905
	O5	2.4663	O6	2.7645	47.431
	O5	2.4663	O6	3.9110	156.105
	O2	2.7355	O6	2.7645	167.476
	O2	2.7355	O1	2.9451	43.854
	O2	2.7355	O6	3.9110	45.808
	O6	2.7645	O1	2.9451	139.841
	O6	2.7645	O1	2.9609	103.240
	O1	2.9451	O1	2.9609	115.526
	O1	2.9451	O3	3.2099	146.973
	O1	2.9609	O5	3.7294	45.394
	O3	3.2099	O5	3.7632	112.476
	O3	3.2099	P2	3.8181	60.469
O4	O3	3.2099	O6	3.9110	144.539
	O4	3.3886	Co1	3.5270	99.147
	O4	3.3886	O2	3.5756	72.211
	Co1	3.5270	P2	3.8181	59.587
	Co1	3.5270	O6	3.9110	67.403
	Co2	3.5398	O2	3.5756	42.407
	Co2	3.5398	P1	3.5878	116.699
	Co2	3.5398	O5	3.7294	133.664
	O2	3.5756	P2	3.8181	146.783
	P1	3.5878	O5	3.7294	19.104
	O5	3.7632	P2	3.8181	171.945
O5	P1	1.2222	O6	2.1215	35.704
	P1	1.2222	Co2	2.3208	123.015
	O6	2.1215	O4	3.7632	163.350
	O6	2.1215	P2	3.8101	86.174
	O6	2.1215	P2	3.8547	108.843
	Co2	2.3208	O4	2.4663	95.320
	Co2	2.3208	Co1	2.4865	118.852
	O4	2.4663	O4	3.7632	102.737
	O4	2.4663	P2	3.8101	95.876
	Co1	2.4865	P2	3.8101	49.940
	Co1	2.4865	P2	3.8547	49.159
	O2	2.5475	O3	2.5520	121.976
	O2	2.5475	O1	2.6771	67.870
	O3	2.5520	O1	3.7359	64.870
	O3	2.5520	O4	3.7632	130.063
	O3	2.5520	P2	3.8101	23.154
	O1	2.6771	P2	3.8101	61.610
	O1	2.6771	P2	3.8547	66.467
	O6	3.0309	O3	3.4479	148.096
	O6	3.0309	P2	3.4562	127.948
	O3	3.4479	O4	3.7632	72.449
	O3	3.4479	P2	3.8101	77.786
	O3	3.4479	P2	3.8547	138.847
	P2	3.4562	O5	3.4814	63.859
	P2	3.4562	O4	3.7294	64.063
	O5	3.4814	P2	3.8101	142.125
	O5	3.4814	P2	3.8547	90.676
	P2	3.6692	O4	3.7294	79.797
	P2	3.6692	O1	3.7359	157.355
	P2	3.6692	O4	3.7632	78.546
	P2	3.6692	P2	3.8101	101.543
	O4	3.7294	O1	3.7359	83.831
	O4	3.7294	O4	3.7632	90.906
	O4	3.7294	P2	3.8101	26.815
	O1	3.7359	P2	3.8547	54.240
	O4	3.7632	P2	3.8101	110.453
	O4	3.7632	P2	3.8547	70.438
	P2	3.8101	P2	3.8547	99.099
O6	P1	1.3354	O5	2.1215	32.284
	P1	1.3354	Co2	2.1694	152.293
	O5	2.1215	O4	3.9110	111.873
	O5	2.1215	O2	3.9416	107.377
	Co2	2.1694	O3	2.5691	110.682
	Co2	2.1694	O4	2.7645	159.226
	O3	2.5691	P1	3.9043	58.958

Table 3. (cont.)

Atom 1	Atom2	d_{1-2} Å	Atom3	d_{1-3} Å	Angle 312
O6	O3	2.5691	O4	3.9110	116.590
	O3	2.5691	O2	3.9416	83.895
	O4	2.7645	O2	2.8042	102.323
	O6	2.7825	P1	3.9043	141.347
	O6	2.7825	O4	3.9110	103.379
	O6	2.7825	O2	3.9416	82.241
	O2	2.8042	O5	3.0309	51.593
	O2	2.8042	O6	3.1627	82.453
	O5	3.0309	O4	3.9110	87.229
	O6	3.1627	Co2	3.3434	158.567
	O6	3.1627	O3	3.3713	46.169
	Co2	3.3434	O4	3.9110	92.220
	Co2	3.3434	O2	3.9416	113.851
	O3	3.3713	P1	3.4154	150.720
	O3	3.3713	P2	3.5725	80.983
	P1	3.4154	O2	3.9416	73.130
	O1	3.7769	O2	3.9416	98.395
	O2	3.8732	P1	3.9043	126.294
	O2	3.8732	O2	3.9416	78.676
	P1	3.9043	O4	3.9110	99.754
	P1	3.9043	O2	3.9416	60.500
	O4	3.9110	O2	3.9416	140.485

distances 3.0353 and 2.9164 Å respectively, which confirms that cobalt has more than one oxidation state over the original common oxidation (CoII and CoIII) inside crystal lattice of cobalt cyclotetraphosphates . This could lead us to informative scientific knowledge that oxidation state of cobalt takes values between Co^{2+}, Co^{m+}, Co^{3+} (where m fractions between 2 ,3 and $2 \leq m \leq 3$). This result may interpret that why the bond lengths of cobalt with six oxygen atoms are different . Plus effect of coupling of charges due to environmental neighboring groups .

Cobalt type two (Co2) has similar behavior to cobalt type one but the oxygen atoms that represent triangle base are recommended to be O2, O5 and O6 with bond lengths 2.5737, 2.3208 and 2.1694 Å, respectively, while axial oxygen atoms could be occupied by O1, O3 and O4 with bond distances 3.5271 ,3.9043 and 3.5398 Å respectively
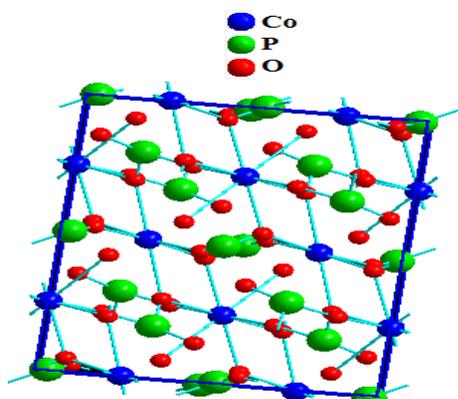
Fig.6 : Unit cell of monoclinic cobalt cyclotetraphosphate .

The cobalt type two (Co2) is also linked with the two different types of phosphorous atoms namely (P1 and P2) with bond distances 3.1577 and 3.7464 Å which confirm that cobalt has more than one oxidation state within the crystal lattice . Similar behavior of existence of multi oxidation states was reported in references [20,21] in which the conditions of synthesis at elevated temperatures in air or oxygen were responsible .
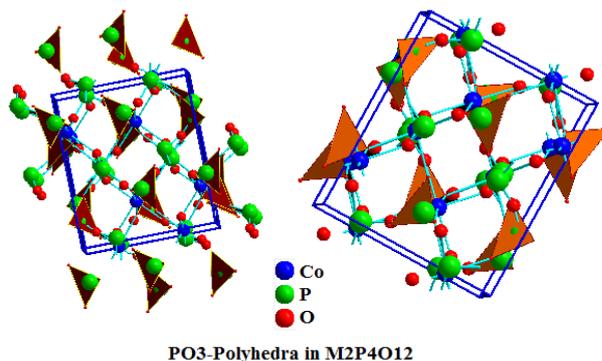
Figure 7 Distribution of PO3-polyhedra in the unit cell of cobalt cyclotetraphosphate .

With respect to phosphorous atoms (P1 and P2) it was observed that phosphorous type one (P1) was linked inside crystal lattice with all oxygen atoms recording bond lengths 1.2222 ,1.3334 and 1.9623 Å correspond to P1-O5 ,P1-O6 and P1-O4 respectively. These bond distances are suitable to be the base triangle of PO3- while the rest three oxygen atoms O1, O2 and O3 recorded bond distances 3.4635 ,3.5532 and 3.3910 which are suited to be axial atoms .

Conclusion

The variations of bond distances between Co1, Co2, P1 and P2 and six different oxygen atoms (O1, O2, O3, O4, O5 and O6) inside crystal lattice are responsible for increasing lattice flexibility factor (by controlling in shrinkage and expansion coefficient) and consequently increase its bonds stability to break. These facts can be attributed to three main factors inside lattice.

1.Oxidation state of cobalt takes values between Co^{2+}, Co^{m+}, Co^{3+} (where m fractions between 2, 3 and $2 \leq m \leq 3$).

2.Effect of coupling of charges due to environmental neighboring groups effects.

3.The six oxygen atoms are liable to replace each other throughout the lattice to compensate any lattice defects could break bonds (evidence is exchanging positions of triangle base with axial positions).

References

[1]Jouini, A., Gacon, J. C., Ferid, M., Trabelsi-Ayadi, M. *Opt. Mater.* **2003**, *24*, 175.

[2]Kitsugi, T., Yamamuro, T., Nakamura, T., Oka, M., *Biomaterials* **1995**, *16*, 1101.

[3]Jian-Jiang, B., Dong-Wan, K., Kug Sun, H., *J. Eur. Ceram. Soc.* **2003**, *23*, 2589.

[4]Martinelli, J. R., Sene, F. F., Gomes, L., *J. Non-Cryst. Solids,* **2000**, *263*, 299.

[5]Parada, C., Perles, J., Saez-Puche, R., Ruiz-Valero, C., Snejko, N. *Chem. Mater.* **2003**, *15*, 3347.

[6]Antraptseva, N. M., Shchegrov, L. N., Ponomareva, I. G., *Russ. J. Inorg. Chem.,* **2006**, *51*, 1493.

[7]Trojan, M., Brandova,´ D., *J. Therm. Anal. Calorim.,* **1985**, *30*, 159.

[8]Trojan, M. *Dyes Pigm.,* **1990**, *12*, 35.

[9]Trojan, M. *Dyes Pigm.,* **1990**, *13*, 1.

[10]Trojan, M., Sÿulcova, P., Mosner, P., *Dyes Pigm.,* **2000**, *44*, 161.

[11]Trojan, M. *Thermochim. Acta,* **1990**, *160*, 361.

[12]Trojan, M., Brandova´, D., *Thermochim. Acta,* **1990**, *160*, 349.

[13]Trojan, M., Sÿulcova, P., *Dyes Pigm.,* **2000**, *47*, 291.

[14]Trojan, M., Brandova, D.; Paulik, F.; Arnold, M., *J. Therm. Anal. Calorim.,* **1990**, *36*, 929.

[15]Trojan, M., Brandova, D., *Thermochim. Acta,* **1990**, *159*, 1.

[16]Brandova, D., Trojan, M., Arnold, M., Paulik, F., *J. Therm. Anal. Calorim.,* **1990**, *36*, 677.

[17]Ramakrishnan, V., Aruldhas, G., *Infrared Phys.,* **1985**, *25*, 665.

[18]Baran, E.J. Mercader, R. C. Massaferro, A. Kremer, E., *Spectrochim.Acta.*, **2004**, *60*, 1001.

[19]Soumhi, E. H. Saadoune, I., Driss, A., *J. Solid State Chem*., **2001**, *156*, 364.

[20]Averbuch-Pouchot, M. T., Durif, A., *Acta Cryst*., **1987,** *C43*, 631.

[21]Chudinova, N. N., Lavrov, A. V., Tananaev, L. V., *Izv. Akad. Nauk SSSR, Neorg. Mater.,* **1972**, *8*, 1971.

[22]Durif, A., Averbuch-Pouchot, M. T., Guitel, J. C, *Acta Cryst*. **1976**, *B32*, 2957.

[23]Enraf-Nonius: Structure Determination Package. RSX 11M version. Enraf-Nonius, Delft, **1977.**

[24]Hilmer, N., Chudinova, N. N., Jost, K. H., *Izv. Akad. Nauk SSSR*, *Neorg. Mat.* **1978**, *14*, 1507.

[25]*International Tables for X-ray Crystallography* (Present distributor D. Reidel, Dordrecht), Vol. IV, Birmingham: Kynoch Press, **1974**.

[26]Palkina, K., Jost, K. H.,Crystallogr., **1975**, *831*, 2285.

[27]Schulz, L., *Z. Anorg. Allg. Chem.* 1956, 287, 106.

[28]Tezikova, L. A., Chudinova, N. N., Fedorov, P. M., Lavrov, A. V., *Izv. Akad. Nauk SSSR, Neorg. Mat.* **1974**, *10*, 2057.

[29]Elsabawy, K. M., Elbagoury, N. H., *Adv. Appl. Science. Res.*, **2011**, *2*(2), 38.

[30]Elsabawy, K. M., *Cryogenics,* **2011**, *51*, 452.